ELSEVIER

CO$_2$ absorption at elevated pressures using a hollow fiber membrane contactor

V.Y. Dindore [a], D.W.F. Brilman [b], P.H.M. Feron [c], G.F. Versteeg [a,*]

[a] *Design and Development of Industrial Processes, Faculty of Chemical Technology, University of Twente, P.O. Box 217, 7500 AE Enschede, The Netherlands*
[b] *Sasol Technology Netherlands B.V., Hallenweg 5, 7522 NB, Enschede, The Netherlands*
[c] *TNO Environment, Energy and Process Innovation, P.O. Box 342, 7300 AH Apeldoorn, The Netherlands*

Abstract

Recently, hollow fiber membrane gas–liquid contactor-based processes have gained an increasing attention. Compared to conventional processes, these processes have numerous advantages. The membrane contactors provide a very high interfacial area per unit volume, independent regulation of gas and liquid flows and are insensitive to module-orientation, which make them very effective in comparison with conventional equipment for offshore application. However, the research done so far is mainly limited to atmospheric pressures applications using aqueous absorption solvents. In this study, the use of hollow fiber membrane contactor for gas absorption at elevated pressure is investigated. CO$_2$ absorption in propylene carbonate was used as a model system in combination with polypropylene (PP) hollow fiber membrane. The absorption experiments were carried out in a semi-batch mode with the solvent continuously flowing through the fiber. The experiments were carried out in a single hollow fiber membrane contactor at elevated pressures up to 20 bar. Higher CO$_2$ pressures result in the increase of the driving force and thus enable higher rates of removal. The study shows that the decrease in the binary gas phase diffusivity and hence the membrane mass transfer coefficient due to increase in the gas pressures does not have a significant effect on the overall mass transfer coefficient. Thus the overall mass transfer coefficient K_o is controlled by the liquid film resistance even at elevated pressures. The overall mass transfer coefficients, at all pressures investigated, can be given by the Graetz–Leveque solution. The long time duration experiments at atmospheric pressure suggest that Accurel PP Q3/2 hollow fiber membrane was subject to morphological changes when used with propylene carbonate as an absorbing solvent. These changes resulted possibly in the wetting of the fiber. It was found that by applying slight over-pressure on the gas-side wetting of the fiber could be avoided and stability of the operation over the long period of application can be obtained.
© 2004 Published by Elsevier B.V.

Keywords: Hollow fiber membranes; Membrane contactors; CO$_2$ absorption; Wetting

1. Introduction

In recent years, gas treating constraints have become more stringent because of higher fuel cost, environmental protection and appearance of CO$_2$ as a large volume product needed in the enhanced oil recovery. The feed gas is usually obtained directly from gas wells with wide range of pressures (normally 2–7 MPa). Depending on the quality of natural gas, it contains varying quantities of CO$_2$ (typically 2–50%). The product of such treating process is an enriched methane stream, containing less than 2% of CO$_2$, sold as a pipeline fuel. The product stream is produced with essentially no pressure loss. A large number of natural gas treating plants around the world are operated with processes based on aqueous solutions of amines and alkali-metal salts. As these solvents chemically react with CO$_2$, to regenerate these solvents, a large amount of heat must be supplied, usually in combination with pressure reduction. These processes become economically unattractive when the CO$_2$ content in the feed gas is high. In the latter cases, usually physical solvents such as propylene carbonate are used for the removal of CO$_2$ [8]. These physical solvents can be regenerated by just the pressure reduction methods without excessive heat inputs. These solvents are especially useful when the partial pressure of CO$_2$ exceeds 1 MPa [17].

Membrane-based gas separation process using dense membrane permeation method are known for their modular design and energy efficiency. The dense membrane

permeation methods have been successfully used for the CO_2 removal for enhanced oil recovery at relatively high pressures [8]. However, at low CO_2 concentrations, CO_2 partial pressure driving force is reduced and significant amount of hydrocarbon (primarily methane) is lost with CO_2-rich permeate. The problem becomes even more severe when other impurities such as H_2S need to be removed as well. The heavy methane loss makes the membrane permeation process economically unattractive in comparison with conventional absorption processes where the selectivity is primarily determined by the absorption liquid. In addition, at high partial pressure of CO_2 the dense membranes used in this process are seriously affected by CO_2 plasticization phenomenon which results in the reduction of selectivity of the process [7].

High separation selectivity (even at low driving force) of the traditional absorption process can be combined with the flexibility, modularity and compactness of membrane process to give a membrane gas absorption process. The contactor used in this membrane gas absorption process to carry out mass transfer operation is generally termed as membrane gas–liquid contactors. This relatively new hybrid process offer several advantages such as higher volumetric mass transfer rates, better selectivity aspects, operational flexibility and easy scale up over the conventional absorption and membrane permeation processes. However, Kreulen et al. [9] showed that the presence of liquid in membrane pores, i.e. wetted mode of operation, significantly reduces the overall mass transfer rate. Therefore it is required that these modules are operated in the non-wetted mode, i.e. pores filled with gases.

In recent years, significant amount of research is carried out to use the membrane gas absorption process for removal of CO_2 from various feed streams. Since hydrophobic membranes are not easily wetted by the aqueous solutions, most of the published work is related to use of the aqueous solvents such as aqueous alkali or alkaline salt solutions which have limited loading of CO_2 due to the chemical nature of these solvents [5]. In addition, the work done with these membrane gas–liquid contactors is limited to low pressure applications. Hence, there is a need of detailed investigation for the use of membrane gas–liquid contactors at elevated pressure and using physical organic solvents for the bulk CO_2 removal.

The membrane contactors have been successfully applied at high pressures (>5 MPa) for dense gas extraction and compressed solvent extraction [2]. The key aspect to operate at high pressures using hollow fibers having burst strength of <500 kPa is the careful control of the pressure on either side of membrane such that although the system pressure is quite high, the pressure drop across the membrane (trans-membrane pressure) is low.

In the present study, application of gas–liquid membrane contactors for the removal of CO_2 from natural gas at elevated pressures is investigated. It was shown earlier that commercial organic solvent propylene carbonate can successfully be used in combination with unused polypropylene hollow fiber for CO_2 removal [4]. Thus the absorption of CO_2 in propylene carbonate at elevated pressure is used as model system in present work. The effects of operating conditions such as pressure, liquid velocity and long-term application are analyzed. The measured mass transfer rates are compared with correlations reported in the literature.

2. Theory

In order to describe a gas absorption into a liquid flowing through a membrane hollow fiber the resistance in series model can be used. Fig. 1 depicts the mass transfer process in the hollow fiber membrane gas–liquid contactor. The overall process consists of three steps. First, the transfer of the solute gas from the bulk gas phase to the membrane surface. Second, transfer through the membrane pores and last, the transfer from the membrane–liquid interface into the bulk of the liquid.

Combined solving of the momentum and diffusion equations is necessary to understand the laminar mass transfer process inside the fiber. The concentration profile in the fiber and the mass transfer rate can be calculated from the differential mass balance equation. Eq. (1) describes diffusion and the forced convection in a hollow fiber membrane. Since the fiber diameter is usually very small, the flow through the hollow fiber is laminar. Axial diffusion is neglected in the equation because the convective transport in the axial direction is much higher than the diffusional transport and the concentration gradient in axial direction is much smaller

$$v_z \frac{\partial C_L}{\partial z} = D \left(\frac{1}{r} \frac{\partial}{\partial r} \left(r \frac{\partial C_L}{\partial r} \right) \right) \tag{1}$$

with boundary conditions

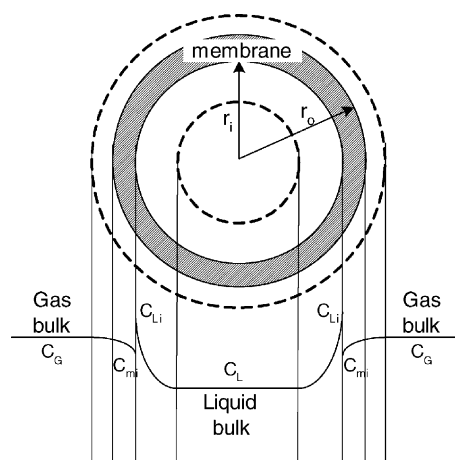$$\left(D \frac{\partial C_L}{\partial r} \right)_{r=r_i} = K_o(mC_G - C_L), \quad 0 \leq z \leq Z$$

Fig. 1. Mass transfer process in membrane G–L contactor.

$$\left(D\frac{\partial C_L}{\partial r}\right)_{r=0} = 0, \quad 0 \le z \le Z$$

The fully developed laminar flow in the hollow fiber can be described by

$$v_z(r) = 2\bar{v}\left(1 - \left(\frac{r}{r_i}\right)^2\right) \tag{2}$$

An analytical solution for this set of differential equations can be obtained when the external mass transfer resistance is very small and can be neglected and if equilibrium exists at the gas–liquid interface. The solution can be derived using the method suggested by Leveque and Graetz [16]. The local value of Sherwood number in terms of Graetz solution is given by Eq. (3) and average Sherwood number is given by Eq. (4)

$$Sh_z = \frac{\sum_{j=1}^{\infty}(B_j/2)(\mathrm{d}\phi_j/\mathrm{d}r^*)_{r^*=1}\exp(-2\beta_j^2/Gz_z)}{2\sum_{j=1}^{\infty}(B_j/2\beta_j^2)(\mathrm{d}\phi_j/\mathrm{d}r^*)_{r^*=1}\exp(-2\beta_j^2/Gz_z)} \tag{3}$$

$$Sh = 0.5Gz\,\theta \tag{4}$$

where

$$\theta = \frac{1 - \sum_{j=1}^{\infty}(-4B_j/\beta_j^2)(\mathrm{d}\phi_j/\mathrm{d}r^*)_{r^*=1}\exp(-2\beta_j^2/Gz)}{1 + \sum_{j=1}^{\infty}(-4B_j/\beta_j^2)(\mathrm{d}\phi_j/\mathrm{d}r^*)_{r^*=1}\exp(-2\beta_j^2/Gz)},$$

$$B_j = 4(j-1) + \frac{8}{3} \ (j = 1, 2, 3, \dots),$$

$$r^* = \frac{r}{r_i}, \quad \frac{B_j}{2}\left(\frac{\mathrm{d}\phi_j}{\mathrm{d}r^*}\right)_{r^*=1} = 1.01276 B_j^{-1/3}$$

The series in the equation for local Sherwood number converges rapidly for small values of Gz, so that only first term is significant. Under these asymptotic conditions the average and the local Sherwood number is given by Eq. (5)

$$Sh = 3.67, \quad Gz < 10 \tag{5}$$

Another asymptotic solution is given by the Leveque equation. Leveque's approximate solution to Eq. (1) is of simpler form and obtained by assuming that the concentration boundary layer is confined to a thin zone near the wall of the fiber. This approximation is valid in cases of high mass velocities through relatively short fibers in laminar flow. One important consequence of this assumption is that the Leveque solution is only applicable for Gz numbers exceeding 20. The Leveque solution is given as

$$Sh = 1.62(Gz)^{1/3}, \quad Gz > 20 \tag{6}$$

It has been shown by many researchers that for systems using aqueous solutions at atmospheric pressures, Graetz–Leveque solution can be used to predict the fiber-side mass transfer coefficient. Kreulen et al. [10] gave the generalized solution of Graetz–Leveque equation by curve fitting of Eqs. (5) and (6), which is also valid for the transition region not covered by Eqs. (5) and (6)

$$Sh = \sqrt[3]{3.67^3 + 1.62^3 Gz}, \quad 10 < Gz < 20 \tag{7}$$

However, membrane contactors for gas absorption in which organic solvents are applied were reported as unstable systems owing to excessive wetting tendencies of the organic solvent [14]. Such systems result in the liquid-filled pores and substantial increase in the mass transfer resistance. In this present study, the absorption of CO_2 in a commercially used physical organic solvent for CO_2 removal (propylene carbonate) in a single hollow fiber membrane module at elevated pressure is investigated. The gas–liquid interface is stabilized at the liquid-side by putting higher pressure on the gas-side of the fiber. It was found that the wetting of the membrane can be effectively prevented by trans-membrane pressure balancing.

3. Experimental

3.1. Materials

Double distilled water and propylene carbonate were used as CO_2 absorption solvents. The propylene carbonate obtained was 99.7% pure and CO_2 and N_2 had 99.99% of purity. Owing to highly hydrophobic nature of polypropylene as a membrane material in combination with its commercial availability, it was decided to use Accurel Q3/2 polypropylene hollow fibers in all experiments. The Q3/2 fiber has an outside diameter of 1000 μm and inside diameter of 600 μm with maximum pore size of 0.64 μm.

3.2. Method

Absorption experiments were carried out in a single hollow fiber membrane contactor. Fig. 2 shows schematically the experimental setup used for the absorption experiments. Two single hollow fiber membrane contactors were used in the experiments. A glass contactor was used for the pressures up to 10 bar and a stainless steel (SS) contactor for higher pressures. Both contactors consisted of a jacketed, cylindrical tube with threaded ends as shown in Fig. 3a and b. The two ends of a membrane hollow fiber were passed through two small stainless steel tubes whose inside diameter was slightly larger than the outside diameter of the hollow fiber. The length of the fiber exposed to the gas during the measurements was the distance between these two SS tubes. The distance between the SS tubes was carefully adjusted and the fiber was potted using epoxy resin to the SS tubes on both the ends of the two tubes. The length of the fiber inside the SS tube ($>0.07\,\mathrm{m}$) on the liquid entry side provides sufficient distance ($>10 d_{in}$) for the laminar liquid profile inside the fiber to be fully developed, before it contacts the gas. The hollow fiber between the SS tubes was placed coaxial to the jacketed tube and the two SS tubes were fastened to the ends of the threaded tube without stretching or putting slack in the fiber. The liquid feed line was connected to the SS tube on the feed side of the contactor. Two vertical glass tubes were attached in the upstream and down stream
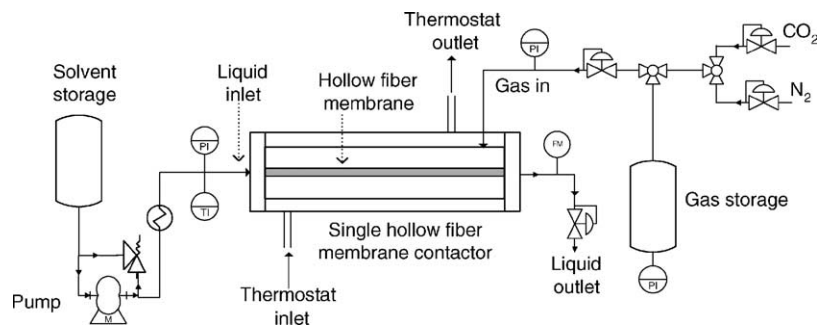
Fig. 2. Experimental setup.

of the liquid feed line so that the gas bubble formation in liquid stream could be observed.

A semi-batch mode of gas–liquid contacting operation was used during the experiments. The liquid flow through the fiber was continuous. The solvent was fed from a high pressure pump via a flow controller. The solvent used in the experiments was degassed before usage by applying vacuum in a separate apparatus. The solvent was passed through the heat exchanger to maintain the desired temperature before entering to the single hollow fiber module. The upstream solvent pressure was controlled using a high precision back pressure controller valve. In all experiments,

sufficient gas pressure was maintained in the contactor before starting the liquid flow. The absence of the gas pressure results in the wetting of the fiber. The CO_2 partial pressure outside the hollow fiber in the contactor was maintained constant by feeding pure CO_2 from a gas supply vessel, through a pressure regulator. From the drop in the pressure of CO_2 in the gas supply vessel, the absorption rate and hence average CO_2 flux across the membrane was calculated:

$$\langle J \rangle = \left(\frac{V}{RT} \right) \left(\frac{1}{\pi d_i l} \right) \left(\frac{P_1 - P(t)}{t} \right) \tag{8}$$
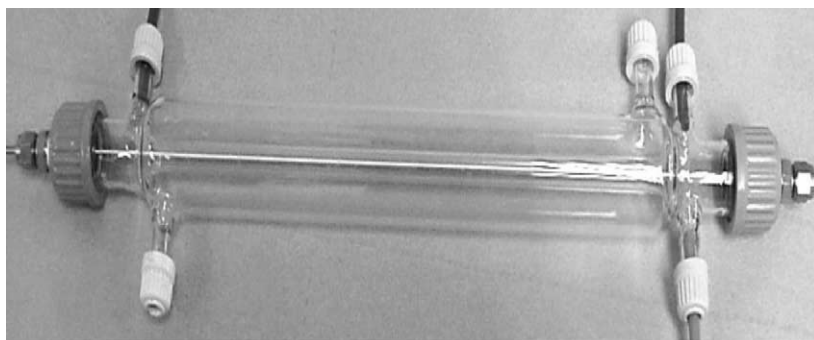
(a)
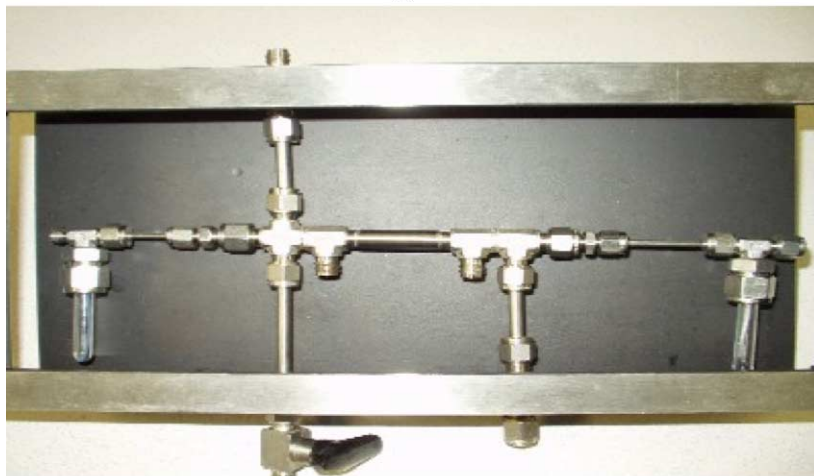
(b)

Fig. 3. (a) Single fiber membrane gas–liquid contactor (glass). (b) Single fiber membrane gas–liquid contactor (SS) with bubble detection tubes.

Table 1
Operating conditions for experiments

No.	System	Operating pressure (bar)	Temperature (°K)	Fiber length (M)
1	PP–water–CO_2	1	293.16	0.27
2	PP–PC–CO_2	1	293.16	0.27
3	PP–PC–CO_2	1.7	293.16	0.15
4	PP–PC–CO_2	2	293.16	0.15
5	PP–PC–CO_2	4.2	298.16	0.13
6	PP–PC–CO_2	8	298.16	0.13
7	PP–PC–CO_2	10	298.16	0.115
8	PP–PC–CO_2	15	298.16	0.135
9	PP–PC–CO_2	20	298.16	0.135
10	PP–PC–CO_2–N_2	8	298.16	0.13
11	PP–PC–CO_2–N_2	4	298.16	0.13
12	PP–PC–CO_2–N_2	4	298.16	0.13

PP: polypropylene hollow fiber, PC: propylene carbonate.

The theoretical average flux can be calculated by a simple mass balance of CO_2 over the length of fiber:

$$\langle J \rangle = \frac{Q_L m C_G (1 - \exp(-K_o \pi d_i l / Q_L))}{\pi d_i l} \qquad (9)$$

The measured flux is then equated to Eq. (9) to calculate the overall mass transfer coefficient K_o. The derivation of Eq. (9) is given in Appendix A. The operating experimental conditions are given in Table 1.

4. Results and discussions

4.1. Absorption in water

Absorption of pure CO_2 in degassed water was carried out in semi-batch mode at atmospheric pressure to test the setup. Pure CO_2 was used to minimize the gas-side mass transfer resistance. In these initial test experiments the liquid-side pressure was maintained higher than that of gas-side pressure in order to avoid the bubble formation in the fiber. The results are shown in Fig. 4. The overall mass transfer coefficient is given as a function of the liquid velocity through the fiber. The figure indicates that the absorption
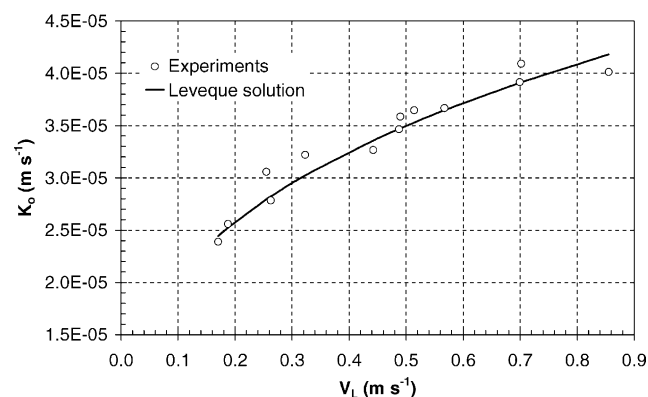
Fig. 4. Effect of liquid velocity on overall mass transfer coefficient for the absorption of CO_2 in water at atmospheric pressure.
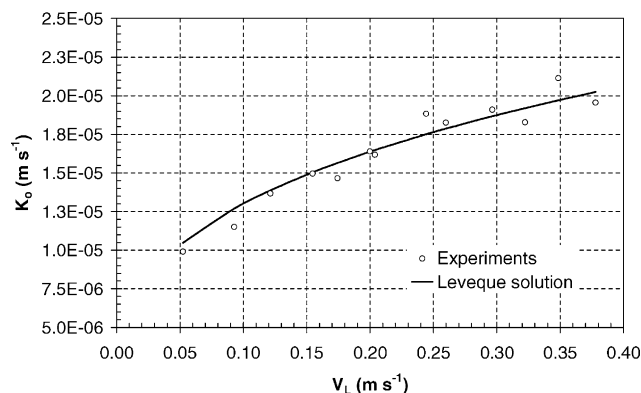
Fig. 5. Effect of liquid velocity on overall mass transfer coefficient for the absorption of CO_2 in propylene carbonate at atmospheric pressure using a new fiber.

rate of CO_2 in water using hollow fiber membrane contactors can be estimated satisfactorily by the Graetz–Leveque equation. In the case of physical absorption in hollow fiber membrane contactors, the controlling resistance for the mass transfer is usually concentrated in the liquid phase. Hence by increasing the liquid velocity, the overall mass transfer coefficient increases. To check effect of the long-term application, water was allowed to run through the fiber for two weeks. At the end of 2 weeks the single hollow fiber contactor showed no decrease in the performance.

4.2. Absorption in propylene carbonate at atmospheric pressure

Initial absorption tests with CO_2 and propylene carbonate were carried out at atmospheric pressure. As recommended in the literature a slight over-pressure was maintained on the liquid-side to avoid the bubble formation. The initial results with virgin membrane are shown in Fig. 5. The overall mass transfer coefficient in this case also can be estimated perfectly with the Graetz–Leveque equation.

It is known that the long-term application of the membrane contactor can affect the morphological characteristics, i.e. hydrophobic nature of the polymeric membranes. Therefore the critical time duration for which membrane contactor can be used without significant decrease in the mass transfer strongly depends on the properties of the liquid phase in the contact with the membrane and the wetting characteristics of the membrane–solvent combination. In addition, the operating conditions such as gas- and liquid-side pressure also affect the mass transfer performance of the membrane contactor. Li and Teo [11] observed that long-term operation of high pressure on the liquid-side resulted into the wetting or partially wetting of the membrane pores. To analyze this effect and also to check the long-term application, propylene carbonate was allowed to run through the fiber for 2 weeks continuously. The absorption experiments were carried out at the end of 2 weeks to check the performance of the membrane
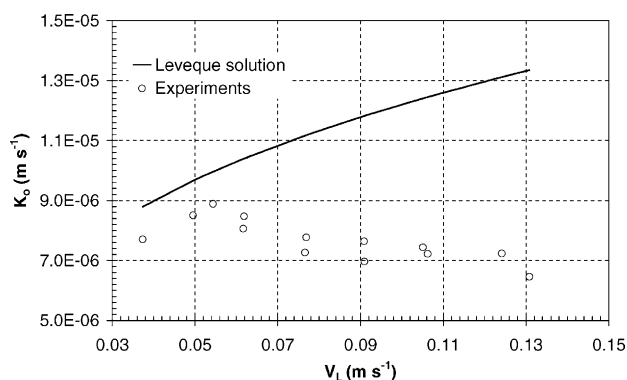
Fig. 6. Overall mass transfer coefficient for the absorption of CO_2 in propylene carbonate at atmospheric pressure after 2 weeks of operation.

contactor. The results are shown in Fig. 6. It is clear from the figure that the performance of the membrane contactor had decreased substantially, most likely owing to the wetting of fiber. As a result the overall mass transfer coefficient obtained is very low. The overall mass transfer coefficient even decreased slightly with an increase in the liquid velocity. This result can be explained by partial wetting of the membrane and indeed the wetting of the membrane was observed during the experimentation and also reported in the literature [12]. Because of the small diameter of the fiber, pressure drop of the liquid inside the fiber lumen will be inevitably increased with increasing liquid velocity and the fiber length according to the Hagen–Poiseuille equation. Since propylene carbonate has a high viscosity compared to water, the pressure drop over the fiber in the case of propylene carbonate is significant, leading to membrane wetting in the initial part of the fiber due to higher pressure gradient over the fiber. This phenomenon can be observed visually by the presence of liquid droplets at the outer surface of the membrane, especially near the inlet of the fiber. The length of the wetted part increases with liquid velocity and thus the average mass transfer coefficient over the length of fiber decreases with the liquid velocity.

SEM analyses were carried out to study the possible changes in the morphology of fiber due to wetting by propylene carbonate. Fig. 7a and b shows the SEM micrographs of the inner surface of the hollow fiber membrane before and after the use, respectively. Although, the detailed morphological changes are difficult to perceive visually in the micrographs, Fig. 7 shows the general roughing of membrane surface after the use. It also can be seen that the number of smaller pores present in the membrane are reduced significantly after the use, while the larger pores seemed to have increased in size slightly. Two possible reasons for these observations could be considered. The first is the intrusion of solvent into larger pores and subsequent enlargement of larger pores. The intrusion into the larger pores is easier than that into the smaller pores. Once larger pores are wetted by the solvent, the additional intrusion into the larger pores exerts lateral force on the pore walls causing the displacement

of these walls. This displacement of the pore walls of larger pores results in the decrease in the size of smaller pores and possibly blocking of these pores. Similar observations were made by Barbe et al. [1] in their recent study about the surface morphological changes induced in microporous membranes due to intrusion of liquid in membrane pores. Another reason could be the contraction of microfibrils due to wetting and subsequent drying of the fiber. This effect was observed by Kamo et al. [6] on wetted-out polyethylene membranes after the contact with various organic solvents. In this case, the pore size was found to increase by an amount that was a function of surface tension of the solvent. It was suggested that the solvent formed a liquid bridge between the microfibrils and that subsequent drying of the solvent then drew the microfibrils sufficiently close together for van der Waals' forces to maintain a more open structure.

Now it seems that the long-term application of high pressure on the liquid-side results in changes in the membrane surface morphology and consequently wetting behavior of the fiber. In order to avoid the wetting Li and Teo [11] applied a thin dense layer on the liquid-side. However, they found that membrane resistance was considerably increased resulting into a low absorption flux. Another possible option to reduce the wetting is to 'push back' the liquid from gas- to liquid-side by applying over-pressure on the gas-side. To verify this idea, experiments were performed using same hollow fiber contactor and gradually increasing the pressure on the gas-side. The results are shown in Fig. 8. This figure shows the experimentally measured absorption flux at various liquid velocities through the fiber. It is clear from the results that with increasing gas-side pressure, the experimental data becomes more in line with the results represented by the Graetz–Leveque equation. At 300 mbar gas-side over-pressure, the experimental values match the theoretical values. During these experiments no bubble formation was observed on the liquid-side. Thus over-pressure on the gas-side can be used to prevent the wetting of the fiber. However, it is important to note that in case of a virgin fiber, over-pressure on the gas-side resulted in the bubble formation. Hence, remaining high pressure experiments were carried out with pre-used fiber and applying a slight over-pressure on the gas-side.

Although the wetting effects can be eliminated by applying an over-pressure on the gas-side, the controllability and the degree of operational freedom is significantly limited. Three different operating conditions can exist depending on the pressure difference between the gas- and liquid-side and the critical wetting and/or bubbling pressure. These three difference cases are shown in Fig. 9a–c. The first case (a) is mostly applicable for the aqueous systems where high pressure is applied on the liquid-side to prevent the bubbling. In this case, high pressure on the liquid-side could result into wetting of initial part of fiber in long-term application. Hence care should be taken that the L–G trans-membrane pressure (P_L–P_G) should not exceed the critical pressure of wetting (ΔP_w) at the liquid inlet. Second case, explained
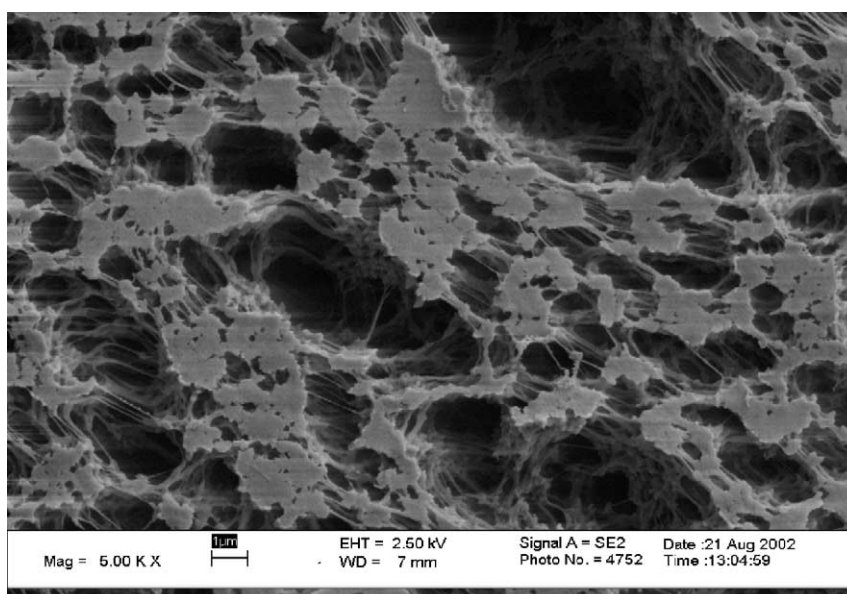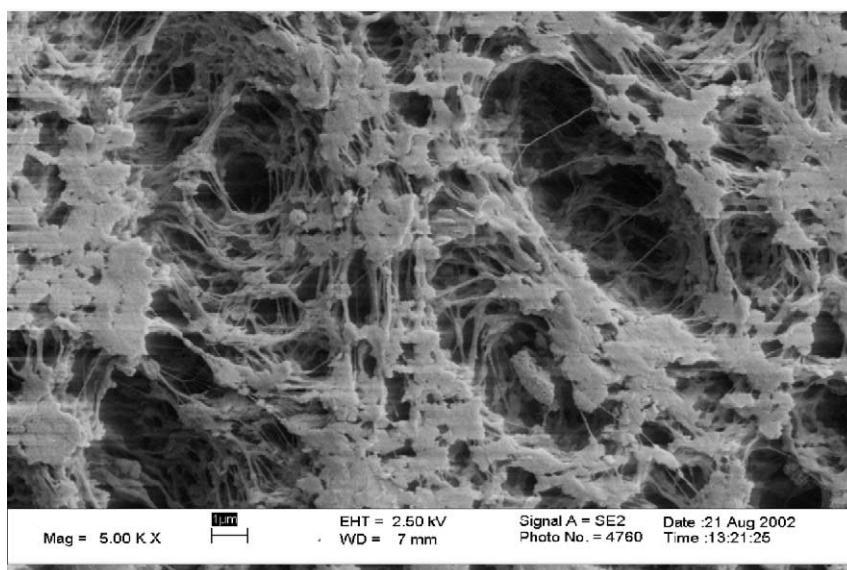
Fig. 7. (a) Scanning electron micrograph of Accurel PP Q3/2 fiber before use. (b) Scanning electron micrograph of Accurel PP Q3/2 fiber after use.

in the Fig. 9b, is applicable for the non-aqueous system where high pressure is applied on the gas-side to prevent the wetting of fiber. In this case, the liquid pressure drop over the fiber leads to bubbling of gas in the liquid stream at the liquid outlet. Hence care should be taken that the G–L trans-membrane pressure (P_G–P_L) should not exceed the critical pressure of bubbling (ΔP_b) at the liquid outlet. In third case, both phenomena can occur simultaneously, i.e. wetting in the initial part of the fiber and bubbling of gas in the end part of the fiber. This situation is illustrated in Fig. 9c. Such case is observed when liquid has intermediate surface tension as compared to aqueous and organic solvents. To avoid these conditions, the L–G trans-membrane pressure (P_L–P_G) in the initial part of the fiber should be lower than the critical pressure of wetting (ΔP_w), where as G–L trans-membrane pressure (P_G–P_L) should not exceed the critical pressure of bubbling (ΔP_b) in the end part of the fiber. These limitations of the operating conditions are illustrated Fig. 10, which gives the qualitative indication of pressure drop control over the fiber. In the figure, solid straight line indicates the $P_G = P_{Lavg}$ line and two dotted lines indicates the two limiting cases of wetting ($P_{Lavg} + \Delta P_w$) and bubbling ($P_{Lavg} - \Delta P_b$) of the fiber, respectively. The four operating lines (case a, case b, case c and case d) show the pressure drop over the fiber, with inlet pressure P_{Lin} being higher than the outlet pressure P_{Lout}. In case (a) (applicable for aqueous system), the high pressure drop over the fiber results into a higher inlet pressure and P_{Lin} crosses the
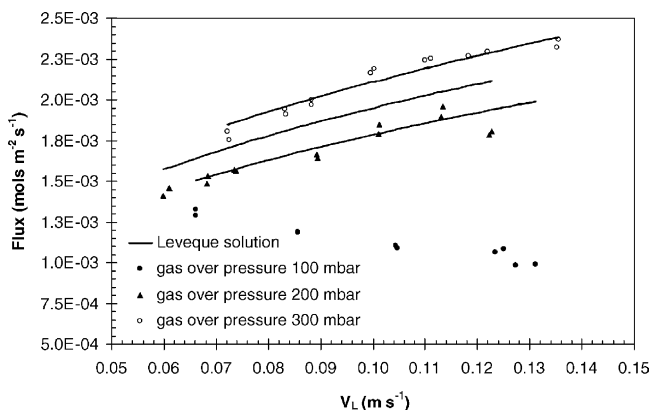
Fig. 8. Effect of gas-side over pressure on CO_2 absorption flux through the hollow fiber in propylene carbonate.

Fig. 10. Operating limitations for membrane G–L contactor.

wetting line causing wetting in the initial part of the fiber. Hence, when high pressure on the liquid-side is applied by controlling liquid outlet pressure, the pressure drop over the fiber should be lower than the critical pressure of wetting (ΔP_w). In case (b) (applicable for the organic systems), the high pressure drop over the fiber results into lower outlet pressure and P_{Lout} crosses the bubbling line causing bubbling in the end part of the fiber. Hence, when high pressure on the gas-side is applied by controlling liquid inlet pressure, the pressure drop over the fiber should be lower than the critical pressure of bubbling (ΔP_b). In case (c) (applicable liquid having intermediate surface tensions), the high
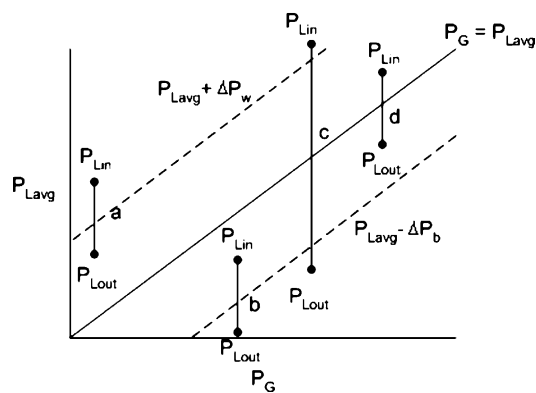
pressure drop over the fiber results in a higher inlet pressure as well as a lower outlet pressure. P_{Lin} crosses the wetting line causing wetting in the initial part of the fiber and P_{Lout} crosses the bubbling line causing bubbling in the end part of the fiber. Case (d) shows the optimum control of the pressure over the fiber. In general, the pressure drop over the fiber should be always lower than ($\Delta P_w + \Delta P_b$). Thus the degree of freedom in the operational conditions becomes limited in such cases and process control turns out to be important.

4.3. Absorption in propylene carbonate at elevated pressure

CO_2 absorption experiments were carried out at elevated partial pressures of CO_2 up to 20 bar with slightly
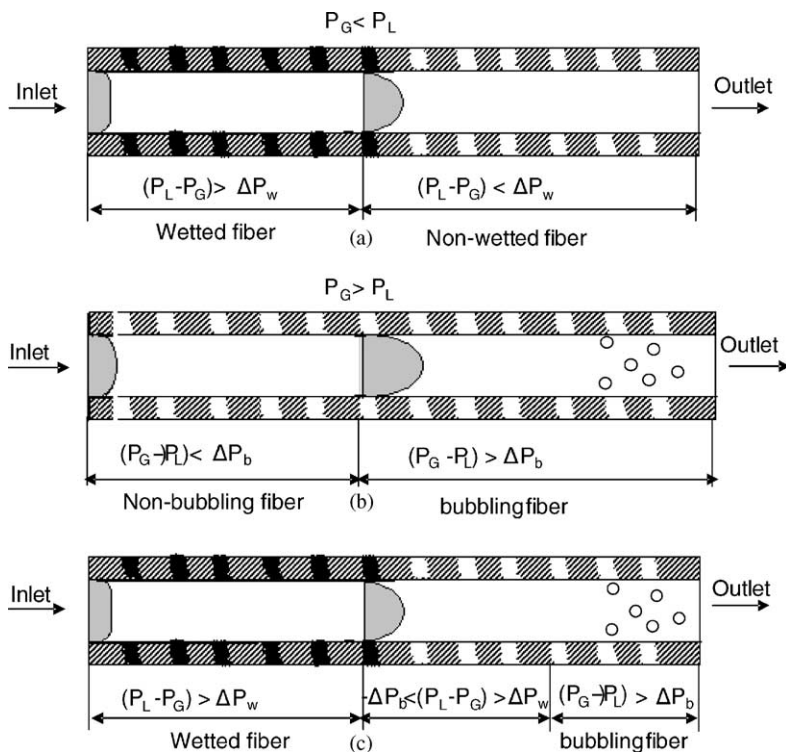

Fig. 9. Microporous hollow fiber membrane operated under: (a) partially wetted mode; (b) partially bubbling mode; (c) partially wetted as well as bubbling mode.
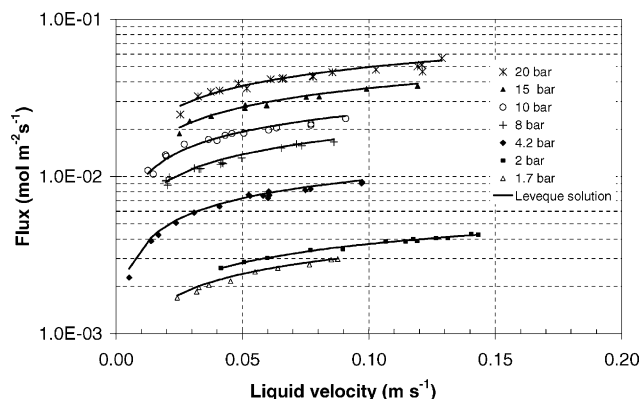
Fig. 11. Measurement of CO_2 absorption flux through the hollow fiber in propylene carbonate at elevated CO_2 pressures.

Fig. 13. Effect of system pressure on the membrane mass transfer coefficient of Q3/2 fiber.

over-pressure on the gas-side. The experiments up to 10 bar were carried out in a glass contactor whereas experiments at high pressure were carried out in a stainless steel contactor. The results are shown in Fig. 11. Measured flux and theoretically calculated flux match very well. The flux at a given liquid velocity increases with pressure. This increase in the flux is due to the increased concentration of CO_2 in the gas phase. Fig. 12 shows the measured mass transfer coefficient (in terms of dimensionless *Sh* number) as function of liquid velocity (in terms of dimensionless *Gz* number) for experiments at all pressures. It is clear the measured mass transfer coefficient can be predicted using the Graetz–Leveque equation, even at elevated pressures. It can be concluded from these figures that there is no effect of pressure on the overall mass transfer coefficient.

At low to moderate pressures, binary gas diffusion coefficients vary inversely with pressure or density of a gas mixture. Thus in case of a binary gas mixture the increase in the pressure results in a decrease in the gas phase diffusivity and hence a decrease in the gas-side and membrane mass transfer coefficients. Fig. 13 shows the effect of pressure on the calculated membrane mass transfer coefficient of the Q3/2 fiber for CO_2–N_2 binary mixture [13]. It is
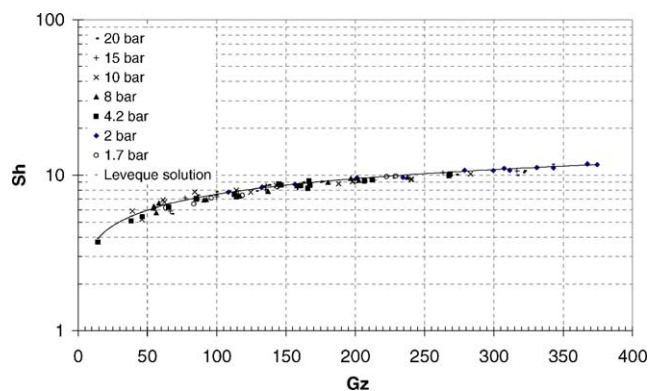
clear that with an increase in the system pressure there is a significant decrease in the membrane mass transfer coefficient. To check this effect of decrease in the membrane mass transfer coefficient on the mass transfer performance of the fiber, experiments were carried out using CO_2 and N_2 binary mixture. The results are shown in Fig. 14. It can be seen that there is no influence of the decrease in the membrane mass transfer coefficient on the overall mass transfer performance. This is because in the case of physical absorption, the liquid-side mass transfer resistance is much higher than the membrane mass transfer resistance. The percentage contribution of membrane and gas phase mass transfer resistances together to the overall mass transfer resistance is very low ($<0.5\%$), even at the higher pressures. Hence the controlling mass transfer resistance still lies in the gas diffusion into the liquid phase and since the pressure has no effect on this process, the overall mass transfer coefficient is independent of the total system pressure. It should be noted that in case of mass transfer with chemical reaction, with a lower liquid-side mass transfer resistance due to the chemical enhancement, increase in the gas and membrane mass transfer resistances at high pressures may significantly affect the results.

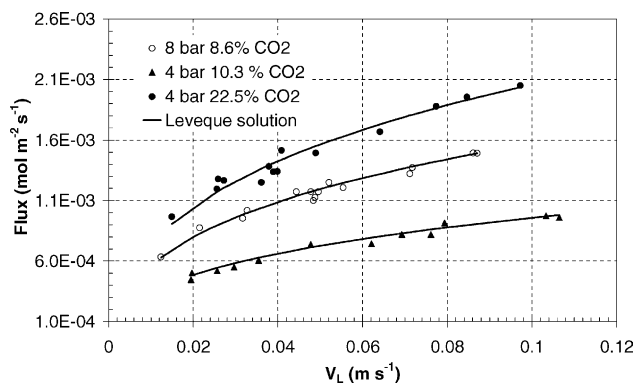Fig. 12. Measurement of overall mass transfer coefficient for the hollow fiber at elevated pressures.

Fig. 14. Measurement of CO_2 absorption flux through the hollow fiber in propylene carbonate at elevated pressures for CO_2–N_2 binary gas mixtures.

5. Conclusion

Absorption of CO_2 in propylene carbonate, a commercial physical organic solvent used in the CO_2 removal process, is investigated in a hollow fiber membrane contactor. The experimental study shows that in the case of physical absorption the overall mass transfer is controlled by the liquid-side mass transfer resistance. Duration experiments at atmospheric pressure suggest that the Accurel PP Q3/2 hollow fiber membrane seems to be subjected to morphological changes when used with propylene carbonate as an absorbing solvent. These changes eventually result in the wetting of the fiber. The wetting problem in long-term application can be avoided by applying over-pressure on the gas-side. However, in such case the pressure drops over the fiber length becomes a critical design parameter to ensure a non-wetted mode of operation. Higher pressure drop over the fiber may lead to wetting in the initial part of the fiber and too high gas-side pressure may result in to the bubble formation in the liquid phase.

The experiments carried out at elevated pressure suggest that membrane gas–liquid contactors can be applied for high pressure applications. The overall mass transfer coefficient is found to be independent of the system pressure. The Graetz–Leveque equation can be used to predict the mass transfer coefficient in a single fiber even at elevated pressures.

Nomenclature

C	concentration (mol/m^3)
d	diameter (m)
D	diffusivity (m^2/s)
Gz	Graetz number, vd^2/Dz
J	flux (mol/m^2 s)
K	mass transfer coefficient (m/s)
l	length (m)
m	distribution coefficient
P	pressure (Pa)
Q	flow rate (m^3/s)
r	radius (m)
R	gas constant
Sh	Sherwood number, $K_l d/D$
t	time (s)

T	temperature (K)
v	velocity (m/s)
V	volume (m^3)
z	length (m)

Subscripts

b	bubbling
G	gas
i	interface/inside
in	inlet
L	liquid
m	membrane
o	overall/outside
out	outlet
w	wetting/water
z	local value

Appendix A. Derivation of flux across the fiber

Since the liquid is continuously flowing through the membrane, the driving force for mass transfer varies with the position in the module. The concentration of CO_2 in the inlet of liquid stream is zero. The concentration of CO_2 in the gas phase is maintained constant by applying constant pressure on the gas-side. As the liquid flows through the fiber, CO_2 is absorbed into the liquid and liquid gets saturated. Thus the driving force for the gas absorption drops with the length of the fiber. An expression for overall flux of CO_2 absorption can be derived by mass balance across a small length of the fiber 'dz' (Fig. 15):

$$0 = Q_L C_L|_{z+dz} - Q_L C_L|_z - J\pi d_i \, dz,$$

$$\text{where } J = k_z(mC_G - C_L) \tag{A.1}$$

The mass transfer coefficient 'k_z' is a clubbed local mass transfer coefficient, taking into account the contribution of the gas-, liquid-side and membrane mass transfer coefficients

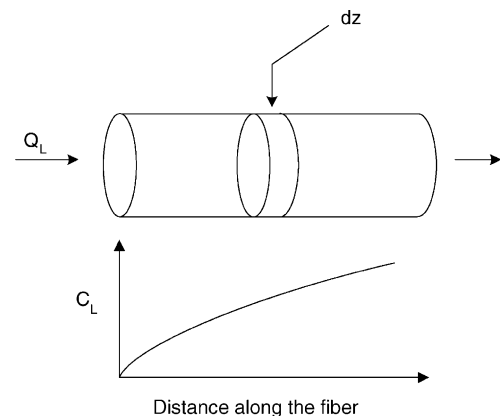$$\frac{dC_L}{dz} = \frac{k_z\pi d}{Q_L}(mC_G - C_L) \tag{A.2}$$

Fig. 15. Mass balance across the small fiber element.

$$\int_0^{C_{Lout}} \frac{1}{(mC_G - C_L)} \, dC_L = \frac{\pi d}{Q_L} \int_0^L k_z \, dz \tag{A.3}$$

Integrating Eq. (A.3) over the entire length of fiber outlet concentration in the liquid stream can be determined

$$C_{Lout} = mC_G(1 - e^{-(k_o \pi d_i/Q_L)L}) \tag{A.4}$$

The mass transfer coefficient 'k_o' is the average clubbed mass transfer coefficient over the entire length of the fiber. Using Eq. (A.4) and taking mass balance for liquid phase, the average flux can be determined:

$$\langle J_{av} \rangle = \frac{Q_L m C_G (1 - e^{-(k_o \pi d_i/Q_L)L})}{\pi d_i L} \tag{A.5}$$

Appendix B. Physical parameters

B.1. Solubility

The solubility of CO_2 in terms of distribution coefficient in pure water, m_w, is taken from Versteeg and van Swaaij [18]

$$m_w = 3.59 \times 10^{-7} RT \exp\left(\frac{2044}{T}\right) \tag{B.1}$$

where R is the universal gas constant (mol m^{-3} K^{-1}) and T is in Kelvin.

The solubility of CO_2 in terms of mole fraction in pure propylene carbonate, x, is taken from solubility data series

$$\ln x = -36.218 + \frac{2856.7}{T} + 3.9003 \ln(T) \tag{B.2}$$

where T is in Kelvin.

B.2. Diffusivity

The diffusivity of the CO_2 and N_2 in water and propylene carbonate is calculated using correlation proposed by Diaz et al. [3]

$$D_{12} = 6.02 \times 10^{-5} \left(\frac{V_2^{0.36}}{\mu_2^{0.61} V_1^{0.64}}\right) \tag{B.3}$$

where V_1 and V_2 are the molar volume at normal boiling point temperature for gas solute and liquid solvent, respectively. μ is the viscosity of the solvent in cP and D_{12} is the diffusivity of solute '1' in solvent '2' in cm^2/s.

The binary diffusion coefficient for the CO_2–N_2 mixture is calculated using Fuller equation [15]

$$D_{AB} = \frac{0.00143 T^{1.75}}{P M_{AB}^{1/2} [(\sum_v)_A^{1/3} + (\sum_v)_B^{1/3}]^2} \tag{B.5}$$

where M_A, M_B are the molecular weights of A and B, $M_{AB} = 2[(1/M_A) + (1/M_B)]^{-1}$, P is the pressure in bar, T is the temperature in Kelvin, $\sum_v$ is the summation of atomic diffusion volumes, D_{AB} is the binary diffusion coefficient in cm^2/s.

References

[1] A.M. Barbe, P.A. Hogan, R.A. Johson, Surface morphology changes during initial usage of hydrophobic, micro-porous polypropylene membranes, J. Membr. Sci. 172 (2000) 197–216.

[2] G.D. Bothun, B.L. Knutson, H.J. Strobel, S.E. Nokes, E.A. Brignole, S. Diaz, Compressed solvents for the extraction of fermentation products within a hollow fiber membrane contactor, J. Supercrit. Fluids 25 (2003) 119–134.

[3] M. Diaz, A. Vega, J. Coca, Correlation for the estimation of the gas–liquid diffusivity, Chem. Eng. Commun. 52 (1987) 271–281.

[4] V.Y. Dindore, Gas purification using membrane gas absorption processes, Ph.D. Thesis, University of Twente, The Netherlands, 2003.

[5] A. Gabelman, S. Hwang, Hollow fiber membrane contactors, J. Membr. Sci. 159 (1999) 61–106.

[6] J. Kamo, T. Hirai, K. Kamada, Solvent induced morphological change of microporous hollow fiber membranes, J. Membr. Sci. 70 (1992) 217–224.

[7] G.C. Kapataidakis, G.H. Koops, M. Wessling, S.P. Kaldis, Sakellaropoulos, CO2 plasticization of polyethersulfone/polyimide gas-separation membranes, AIChE J. 49 (7) (2003) 1702–1711.

[8] A.L. Kohl, R.B. Nielsen, Gas Purification, 5th ed., Gulf Publishing Company, Houston, 1997.

[9] H. Kreulen, C.A. Smolders, G.F. Versteeg, W.P.M. van Swaaij, Determination of mass transfer rates in wetted and non-wetted micro-porous membranes, Chem. Eng. Sci. 48 (1993) 2093–2102.

[10] H. Kreulen, C.A. Smolders, G.F. Versteeg, W.P.M. van Swaaij, Microporous hollow fiber membrane modules as gas–liquid contactor. Part 1. Physical mass transfer processes, J. Membr. Sci. 78 (1993) 197–216.

[11] K. Li, W.K. Teo, An ultra thin skinned hollow fiber module for gas absorption at elevated pressures, Chem. Eng. Res. Des. A 74 (1996) 856–862.

[12] A. Malek, K. Li, W.K. Teo, Modeling of microporous hollow fiber membrane modules operated under partially wetted conditions, Ind. Eng. Chem. Res. 36 (3) (1997) 784–793.

[13] M. Mulder, Basic Principles of Membrane Technology, Kluwer Academic Publishers, Dordrecht, 1996, pp. 149–156.

[14] B.W. Reed, M.I. Semmens, E.L. Cussler, Membrane contactors, in: R.D. Noble, S.A. Stern (Eds.), Membrane Separation Technology, Principles and Applications, Elsevier, Amsterdam, 1995, pp. 467–498.

[15] R.C. Reid, J.M. Prausnitz, B.E. Poling, The Properties of Gases and Liquids, McGraw-Hill, New York, 1987, pp. 577–626.

[16] A.H.P. Skelland, Diffusional Mass Transfer, Wiley, New York, 1974, pp. 159–168.

[17] J.W. Sweny, Gas treating with physical solvents, in: S.A. Newman (Ed.), Acid and Sour Gas Treating Processes, Gulf, Houston, 1985, pp. 1–41.

[18] G.F. Versteeg, W.P.M. van Swaaij, Solubility and diffusivity of acid gases in aqueous alkanolamine solutions, J. Chem. Eng. Data 33 (1988) 29–34.